ELSEVIER

Carbohydrate Research 287 (1996) 21–35

CARBOHYDRATE RESEARCH

Investigation of the α-cyclodextrin–*myo*-inositol phosphate inclusion complex by NMR spectroscopy and molecular modeling

Serge Crouzy [a], Florence Fauvelle [b], Jean-Claude Debouzy [b,*], Mathias Göschl [a], Yves Chapron [a]

[a] *C.E.A. Grenoble, Département de Biologie Moléculaire et Structurale 17, rue des Martyrs, F-38054 Grenoble, France*

[b] *Centre de Recherches du Service de Santé des Armées, Unité de Biophysique, 24 Av. du Grésivaudan, F-38702 La Tronche, France*

Received 24 August 1995; accepted in revised form 4 March 1996

Abstract

$^{1}H-^{31}P$ NMR spectroscopy and molecular dynamics (MD) have been used to investigate the *myo*-inositol 2-phosphate (MY2P) inclusion complex in α-cyclodextrin (α-CD). From spectral analyses, it has not been possible to estimate the stoichiometric ratio of MY2P to α-CD, however several geometrical constraints between the two molecules have been deduced from nuclear Overhauser effects and chemical shift measurements. Based on a MD study, a model for the α-CD–MY2P interaction is proposed showing the possible coexistence of loose and tight inclusion of MY2P into α-CD. © 1996 Elsevier Science Ltd.

Keywords: Cyclodextrin; *Myo*-inositol 2-phosphate; NMR spectroscopy; Molecular dynamics; Inclusion complex

1. Introduction

Of the cyclomaltooligosaccharides, cyclomaltohexaose (α-cyclodextrin, α-CD), interacts strongly with long-chain alkanes and long-chain surfactants [1,2]. This has led to the proposal of a non-specific lipid extraction from the membrane as the mechanism responsible for the hemolytic activity of α-CD [2]. In a previous report [3], however, we

* Corresponding author.

PII S0008-6215(96)00058-4

have shown that such a non-specific scheme of interaction with phospholipids is at least incomplete, since the nature of the headgroup of the phospholipid appears to be a determining criterion for its association with α-CD. Furthermore, of the different species tested, the phospholipids bearing an inositol group have been found to exhibit the highest affinity for α-CD [4]. Thus, in addition to the probable chain inclusion into the α-CD cavity [5], another interaction must occur between an α-CD molecule and the inositol moiety.

In the present report, the interaction of α-CD and *myo*-inositol 2-phosphate (MY2P), the polar group of inositol phospholipids, is investigated by NMR spectroscopy and molecular modeling. In a first step, the formation of the complex is studied by ^{1}H and ^{31}P NMR spectroscopy in aqueous solution and nOe distances are deduced from these experiments. In a second step, a molecular dynamics study of the α-CD–MY2P interaction is performed and molecular models are proposed for the complex formation satisfying the previous nOe restraints. Although not frequent, this kind of interaction between cyclodextrins and polar entities have already been reported by other authors [6].

2. Experimental

General.—*myo*-Inositol 2-phosphate and α-cyclodextrin were purchased from Sigma (Saint Quentin Fallavier, France) and used without further purification.

Inclusion complex preparation.—The α-CD and MY2P structures were first studied in aqueous solution in D_2O at 297 K (2 mM), pH 7. The molecular ratios used for the formation of complexes were determined following the Job-plot method [7,8]: stock solutions (20 mM) of α-CD and MY2P were used and mixed in the NMR tube in various molecular ratios to yield a final total concentration (α-CD + MY2P) of 4 mM. The resulting mixtures were lyophilized and finally resuspended in 500 μL D_2O.

NMR spectroscopy.—^{1}H NMR experiments were recorded at 400 MHz using a AM400-NB Bruker spectrometer. Standard COSY, 1D-nOe and 2D-NOESY experiments (variable delay of 0.4s) were used [9]. ^{31}P NMR spectra were recorded at 162 MHz with a AM400-WB Bruker spectrometer without proton decoupling. All the spectra were recorded at 297 K.

Molecular modeling.—The initial α-cyclodextrin (α-CD) coordinates of all non-hydrogen atoms were taken from crystallographic data of α-CD [10]. In cyclodextrin, three hydroxyl groups per glucose residue provide donors and acceptors for hydrogen-bonding-based stabilization of the macrocycle and the possibility of a flexible bonding scheme for other organic compounds in contact with α-CD [11].

For *myo*-inositol phosphate (MY2P), coordinates were taken from *myo*-inositol-anhydrate [12,13] for the inositol component. Equilibrium values for dihedral angles in the phosphate inositol linkage were set to the values proposed by Hansbro et al. [14] yielding a MY2P structure used for all the subsequent simulations. The total charge of α-CD is 0 whereas the total charge of MY2P, predominantly located on the phosphate group, is −1. A sketch of the two molecules is shown. (Proton numbering of α-CD and MY2P. Proton numbers are indicated for all hydrogens bonded to a C atom. Protons of MY2P are primed to distinguish them from α-CD protons.)

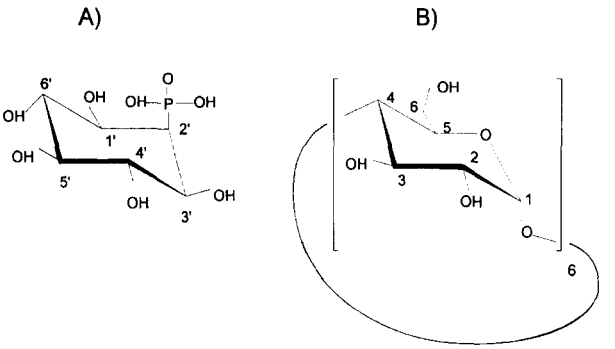

Computational methods.—Building of the structure and MD simulations were carried out using the CHARMM [15] force field. Missing hydrogen atoms were added using the CHARMM HBUILD command with default settings. The SHAKE [16] method was applied to constrain bond lengths involving hydrogen atoms to cancel rapid X–H vibrations (where X stands for a heavy atom). Dynamic runs were performed using the Verlet algorithm with a 1 fs integration step. Due to the relatively small number of atoms in the system, velocity rescaling with $\tau = 0.5$ ps coupling to a $T_{ref} = 300$ K

Table 1
Partial charges of α-CD and MY2P

α-CD [a]		MY2P			
Atom	q	Atom	q	Atom	q
C-1	0.1338	C-1	0.1734	P	1.3192
C-2	−0.0196	C-2	0.0761	O-11	−0.5092
C-3	−0.0101	C-3	0.1109	O-12	−0.5868
C-4	0.0104	C-4	0.1084	O-13	−0.7755
C-5	−0.0174	C-5	0.1350	O-14	−0.7354
C-6	−0.0153	C-6	0.0972	HZZ	0.1811
O-2	−0.3244	H-1	0.0067		
O-3	−0.3340	H-2	0.0264		
O-4	−0.3080	O-2	−0.3463		
O-5	−0.2921	H-3	0.0412		
O-6	−0.3276	O-3	−0.3284		
H-1	0.1438	H-4	0.0143		
H-2	0.1321	O-4	−0.3168		
H-3	0.1185	H-5	0.0137		
H-4	0.1163	O-5	−0.3276		
H-5	0.1151	H-6	0.0103		
H-21	0.2343	O-6	−0.3460		
H-31	0.2267	H-12	0.2020		
H-61	0.1162	H-13	0.1840		
H-62	0.0842	H-14	0.1755		
H-63	0.2169	H-15	0.1862		
		H-16	0.2105		

[a] Charges are the same for all six identical glucose residues.

heatbath was used to perform constant temperature dynamics [17]. Non-bonded interaction cutoff was set to 15 Å. The partial charges of α-CD were calculated using the semi-empirical orbital approximations of the MOPAC program with MNDO hamiltonian [18,19]. By repeated steps of Adopted-Basis-Newton–Raphson (ABNR) minimization [15] and partial charges reevaluation (MOPAC geometry optimization was disabled), the structure converges to a charge distribution similar to that present in the CHARMM/QUANTA parameter set for single glucose residues but taking into account the particular topology of α-CD. For MY2P, the topology of the phosphate group was taken from the CHARMM22 library file: *top_all22_lipid*, for DLPE (dilauryl phosphatidylethanolamine) and the topology of the inositol group from QUANTA/Chemnote. The charge distributions of both groups were calculated with MOPAC. Final charges are given in Table 1. Force constants and non-bonded interaction parameters for MY2P were taken from the CHARMM22 parameter file *par_all22_lipid* where the inositol group and its link to the phosphate group were parameterized with the standard settings available in this file. For α-CD, the force field parameters were taken from the QUANTA/Chemnote library files for the glucose molecules and the glycosidic bond parametization was done using default values of the same files that are found to be close to the force field proposed by Koehler et al. [20].

The α-CD molecule was first oriented with its principal axis aligned with the *z*-axis and its mass center positioned at the origin of the coordinate system. The main axis of MY2P was also aligned with the *z*-axis. For all simulations, the center of mass of α-CD was fixed to prevent rigid body translation of the system. Four different structures for the complexation between MY2P and α-CD were considered, (Fig. 5): with (a), the phosphate group of MY2P facing the secondary hydroxyl side of α-CD; (b), the inositol group of MY2P facing the primary hydroxyl side of α-CD; (c), the phosphate group of MY2P facing the primary hydroxyl side of α-CD and (d), the inositol group of MY2P facing the secondary hydroxyl side of α-CD.

Vacuum simulations.—Initial structures corresponding to the four schemes presented in Fig. 5 were built 'manually' using QUANTA by translating and rotating MY2P and α-CD as rigid bodies. Then, each structure was energy minimized in vacuum using CHARMM: one atom of α-CD was fixed, namely O-4 from residue 1, to prevent α-CD from tilting aside or freely rotating around its principal axis. First, small harmonic restraints were placed on all MY2P atoms to prevent them from being pushed very far away from the initial structure, due to possible strong Van der Waals (VDW) contacts, and 100 steps of ABNR minimization were done. Then, after removing the harmonic restraints, 1000 steps of ABNR minimization were run and the final coordinates saved. MD trajectories were computed starting from these energy minimized structures. Heating from 0 to 300 K in 3 ps was followed by 5 ps equilibration and 50 ps production dynamics at 300 K. Coordinates of all atoms were saved to a trajectory file for further analysis every 50 fs.

Simulations in the presence of water.—Before solvating the system, 1000 steps of ABNR minimization were performed following the same protocol as in the previous section, for all four configurations starting from the average atomic coordinates calculated from the vacuum simulations. The resulting energy minimized structures were then solvated by inserting them into a 12 Å radius sphere of equilibrated TIP3S water

molecules [21] provided by QUANTA and deleting all water molecules closer than 1.8 Å to a heavy atom of MY2P or α-CD. For all subsequent solvent simulations, a spherical boundary potential [22] for water molecules was introduced to keep them inside the sphere centered at the origin. The solvated structures (α-CD + MY2P + 197 to 201 water molecules) were then energy minimized. Again, one oxygen atom from α-CD was fixed and harmonic restraints first applied on all MY2P atoms were removed after 200 steps ABNR minimization and prior to 1500 steps of final minimization. This procedure was repeated for six possible initial configurations of MY2P inside α-CD obtained after rotating MY2P around its principal axis z, from 0 to 300 degrees in steps of 60 degrees. For each configuration (a) to (d), the structure with minimum energy after all rotations and minimizations was used as a starting point for dynamics calculations. After heating and equilibration at 300 K in the same manner as for the vacuum simulations, production dynamics lasting from 200 to 400 ps were computed; 200 ps for configurations (c) and (d), 300 ps for (b) and 400 ps for (a). These different times come from the fact that simulations were restarted until electrostatic interaction energy between α-CD and MY2P was judged stationary in each case.

3. Results

^{1}H NMR study of the α-CD–MY2P inclusion complex.—^{1}H NMR peak assignment (see proton numbering in structure above) was achieved as follows using COSY experiments, according to previous work [23,24]. For MY2P (2 mM, D_2O), H-2′ (1 H, 4.34 ppm, tt), H-1′,3′ (2 H, 3.31 ppm, dd), H-4′,6′ (2 H, 3.57 ppm, t), H-5′ (1 H, 3.11, t). For α-CD (2 mM, D_2O), H-1 (6 H, 4.91, d), H-3 (6 H, 3.84, t), H-2 (6 H, 3.51, dd), H-4 (6 H, 3.42, t), H-5,6 (18 H, overlapped multiplets in the 3.6–3.8 ppm region). The ^{1}H NMR spectrum of α-CD (2 mM, 297 K, D_2O) is shown in Fig. 1B. As α-CD is a symmetrical hexamer, the intensity of each resonance is enhanced by a factor of six compared to the MY2P signals at the same concentration. At this stage, it is important to recall that the α-CD molecule adopts the conformation of a torus where H-3 and H-5 protons are located inside the cavity, while H-2 and H-4 are outside the torus and in contact with the aqueous medium [10]. The H-6 protons of the primary alcoholic group are on the narrow side and H-1 in the glycosidic bond plane of α-CD. The spectrum recorded under the above-described conditions with an equimolar solution of α-CD and MY2P is shown in Fig. 1A. By comparison with the spectrum of pure α-CD, several chemical shift variations appear: H-3, H-5 and H-6 resonances are upfield shifted by 6, 4 and 3 Hz, respectively, while H-2, H-4 and H-1 signals are unaffected (H-1 resonance not shown). On the other hand, the H-2′ and H-1′,3′ resonances of MY2P are downfield shifted, by −10 Hz and −12 Hz, respectively, while the H-4′,6′ peak is slightly affected (−2 Hz) and the H-5′ resonance remains unaffected. These features reveal that the protons of α-CD affected by the presence of MY2P are located inside the torus (H-3,H-5) or at the narrow side (H-6) of the molecule. Similarly, significant shifts are found for the protons located in the region of MY2P bearing the phosphate group (H-1′, H-2′, H-3′). As discussed in the literature [25,26], these results suggest a more or less complete inclusion of the MY2P molecule in the cavity of α-CD. This led us to prepare

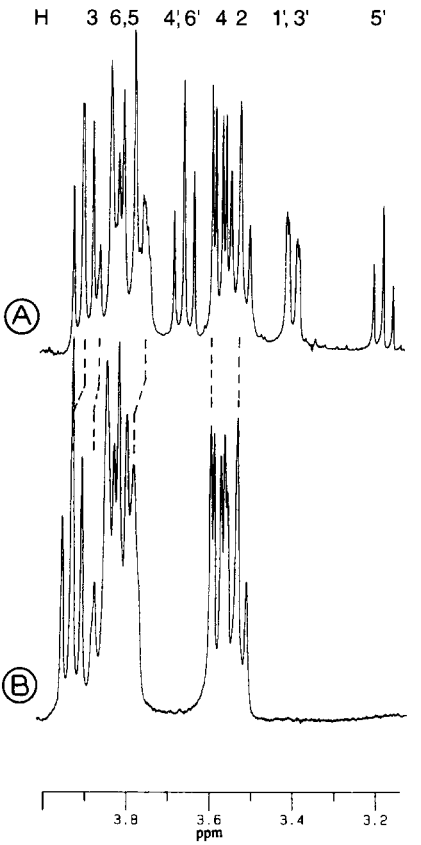

Fig. 1. α-CD interactions with MY2P. ^{1}H NMR (400 MHz) spectra of: (A) an equimolar preparation of MY2P–α-CD (2 mM, 297 K, D_2O), see proton nomenclature; (B) of pure *myo*-inositol 2-phosphate (2 mM, D_2O, 297 K). The chemical shift variations of the resonances due to interacting protons are figured with dashed lines; The H-1 resonance of α-CD is not shown.

complexes of various α-CD/MY2P molar ratios to keep the total concentration constant using the method of Job [7,8], by lyophilization of the mixture followed by resuspension in D_2O.

Molar ratio dependence of the α-CD–MY2P inclusion complex.—The chemical shift variations of H-3, H-5, H-6 resonances of α-CD as a function of its molar fraction are shown in Fig. 2. These curves are generally drawn to determine the stoichiometry of a complex, which corresponds to the maximum of the curve. Such a result could not be obtained in the case of α-CD–MY2P: highfield shifts of H-3, H-5 and H-6 resonances increase with MY2P ratios without reaching any maximum or steady state in the curve (the maximum value observed was 27 Hz for H-3 and H-5 and 10 Hz for H-6 peaks, for an α-CD/(MY2P + α-CD) ratio of 1/100). Furthermore, a quite different concentration dependence was observed for MY2P resonances: low amounts of α-CD (α-CD/(MY2P + α-CD) of 5/100 or less) were sufficient to induce observable shifts of H-1′,3′ and H-2′ resonances and to reach a plateau value of − 10 Hz (not shown) so that

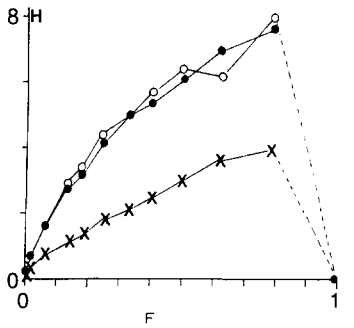

Fig. 2. Job-plot study of α-CD–MY2P interactions. ^{1}H NMR (400 MHz: chemical shift variations of H-3 (●), H-5 (○) and H-6 (×) resonances weighted by [α-CD] (mM) as a function of [α-CD]/[α-CD + MY2P] molar ratio. The total concentration [MY2P] + [α-CD] in the sample was 4 mM.

no stoichiometric information could be drawn from these experiments. In order to confirm the existence of a MY2P inclusion, it was then of interest to record ^{31}P NMR spectra on the same samples. The undercoupled ^{31}P NMR spectrum of MY2P (2 mM) in aqueous solution is shown in Fig. 3 (bottom right). The observation of less than 2 Hz linewidths is in good agreement with the solubility of MY2P, whereas a 7 Hz coupling constant J_{POCH_2} suggests a gauche dominant conformation as described elsewhere [27].

Upon complex formation, such coupling constants are no more observable (even for

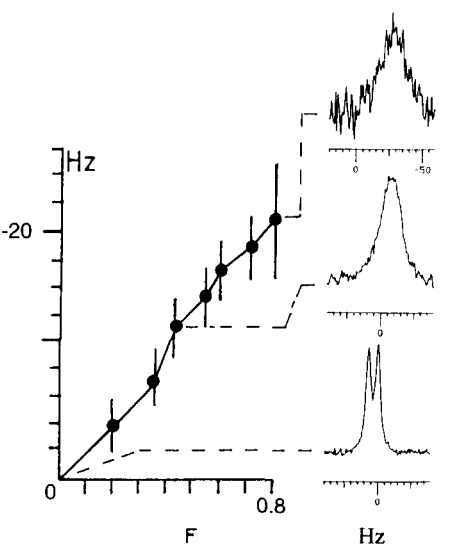

Fig. 3. ^{31}P NMR (162 MHz) study of 1 α-CD–MY2P interactions. Chemical shift variations (Hz) of the ^{31}P NMR resonances of MY2P as a function of [MY2P]/[MY2P + α-CD] molar ratios and corresponding spectra of pure MY2P (4 mM, D_2O, 297 K, bottom right); of an equimolar α-CD–MY2P preparation (middle right); and of a 10% [MY2P]/[MY2P + α-CD] preparation (top right). The chemical shift differences were measured using the spectra of pure PI at the same concentration as references.

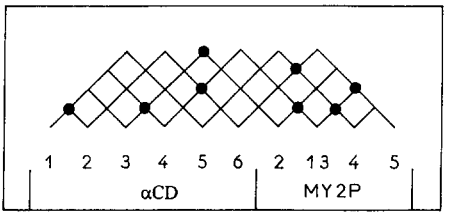

Fig. 4. Dipolar connectivities between α-CD and MY2P. ^{1}H NMR (400 MHz) NOESY experiment (mixing time of 400 ms). Each diagonal line corresponds to the proton resonance place at the bottom. The dipolar connectivities observed on an equimolar preparation of α-CD and MY2P (total concentration of 4 mM, 297 K) are figured by filled circles (●) at the crossing of the lines.

1:10 α-CD–MY2P molar ratios, as shown on the spectra at the top and middle right part of Fig. 3) while a broad resonance is found at an upfield position. A concentration dependence of the ^{31}P NMR spectra of MY2P was first rejected by comparison with spectra recorded at the same concentrations using pure MY2P. The broadening and shifting of the phosphorus resonance were then found to increase upon α-CD addition, up to 23 and 25 Hz, respectively. However, the chemical shifts for high α-CD/MY2P molar ratios are very inaccurate due to the weakness of the signal and its intrinsic width. Such broadening effects (T_2 shortenings) occur when the mobility of a molecule is limited by the formation of an aggregated form and/or when the molecule is involved in an inclusion process. After checking that no induced variation of pH was measured according to data in the literature [8,10], another argument in favor of the inclusion of MY2P was obtained by recording ^{31}P NMR spectra of MY2P in apolar or hydrophobic solvents. Indeed, broad resonances were found at highfield, both in dimethyl sulfoxide (50 Hz linewidth at 80 Hz highfield) and in octanol (20 Hz linewidth at 130 Hz highfield). By considering both molecules, the only hydrophobic environment can be

Table 2
Minimum H–H distances [a]

Structure	Vacuum			Solvent		
	α-CD	MY2P	(Å)	α-CD	MY2P	(Å)
(a)	H-3^{IV}	H-2′	2.41	H-3^{IV}	H-2′	2.31
	H-62^{IV}	H-4′	5.12	H-61^{IV}	H-4′	4.88
(b)	H-3^{II}	H-2′	5.85	H-3^{II}	H-2′	7.38
	H-61^{III}	H-4′	2.30	H-62^{III}	H-4′	2.29
(c)	H-3^{IV}	H-2′	7.89	H-3^{VI}	H-2′	8.21
	H-61^{V}	H-4′	5.05	H-62^{V}	H-4′	4.77
(d)	H-3^{I}	H-2′	3.07	H-3^{V}	H-2′	4.11
	H-61^{I}	H-4′	5.29	H-62^{VI}	H-6′	5.30

[a] Distances for which dipolar connectivities have been detected by nOe experiments, i.e. H-3 to H-2′ or H-6 (2 protons) to H-4′ (see Fig. 5). The distances between H-6 and H-6′, always larger than H-6 to H-4′, are not reported.

found in the α-CD cavity. Furthermore, it clearly appears that the resonances of the phosphorus atom, on the ^{31}P NMR spectra, and of H-2′,1′,3′, on the ^{1}H NMR spectra, are high-field shifted and that the corresponding nuclei are probably included in the α-CD torus while H-4′,5′,6′ are not. However, a direct explanation of the chemical shift dependence on the molar ratios lacks at this stage. The hypothesis of a partial inclusion of MY2P into the α-CD cavity may be consistent with a mechanism of association more complex than a single inclusion process. Indeed, if one considers the negative charge of the phosphate and the hydroxyl groups of both inositol and α-CD, a hydrogen bond mediated association can exist between MY2P and the external part of the α-CD torus. In the case of a nitroxide–cryptophane association, investigations have shown [28] that both more or less competing mechanisms can coexist and give rise to uninterpretable Job-plots. Intermolecular constraints were then derived from NOESY experiments (mixing times from 100 to 400 ms). In the absence of both canonical distances and of acceptable mean value for T_1 (i.e. for α-CD: 400 ms for H-5 and H-6, 600 ms for H-4, and 1.2 ms for H-2 and H-3), no precise proton–proton distances could be deduced. This led us to propose the grid diagram in Fig. 4 derived from spatial connectivities obtained with an equimolar preparation. In addition, the expected intramolecular correlations, (H-1–H-2, H-3–H-4, H-4–H-6 for α-CD, and H-2′–H-1′,3″, H-1′,3′–H-4′,6′, H-1′,3′–H-5′ for MY2P), several intermolecular constraints were observed, especially between the interacting protons, α-CD–H-3 and MY2P–H-2′, and α-CD–H-6 and MY2P–H-4′,6′. It should be underlined that, if the first correlation is in agreement with an inclusion process, the latter is not exclusive of an external association between the two moieties. These elements were then used in association with crystallographic data and MD calculations to build a model of the α-CD–MY2P complex.

Molecular models.—A summary of average H–H distances between α-CD and MY2P measured from MD trajectories is given in Table 2. MD simulations in the presence of solvent were first run for 50 ps as in the case of vacuum simulations and then extended to 200 or 400 ps, depending on the configuration, to allow a better sampling of the positions of water molecules. Average structures and H–H distances during these simulations turned out to be very similar to those obtained in the shorter ones. Some of these distances are reported in Fig. 5 which shows average structures obtained after 200 ps MD simulations. Average energies calculated from these dynamics runs are summarized in Table 3: from E_{Inter}, the interaction energy between α-CD and

Table 3
Average energies during 200 ps

Structure	E_{Inter} [a] (kcal/mol)	E_{Solv} [b] (kcal/mol)	E_{Tot} [c] (kcal/mol)
(a)	−56.7	−22.8	−1838.9
(b)	−20.5	−61.9	−1821.5
(c)	−29.2	−46.7	−1821.5
(d)	−26.4	−65.5	−1848.0

[a] E_{Inter}: Interaction energy α-CD–MY2P.
[b] E_{Solv}: Total interaction energy α-CD–MY2P + α-CD–Solv + MY2P–Solv.
[c] E_{Tot}: Total potential energy = E_{Solv} + Solv–Solv.

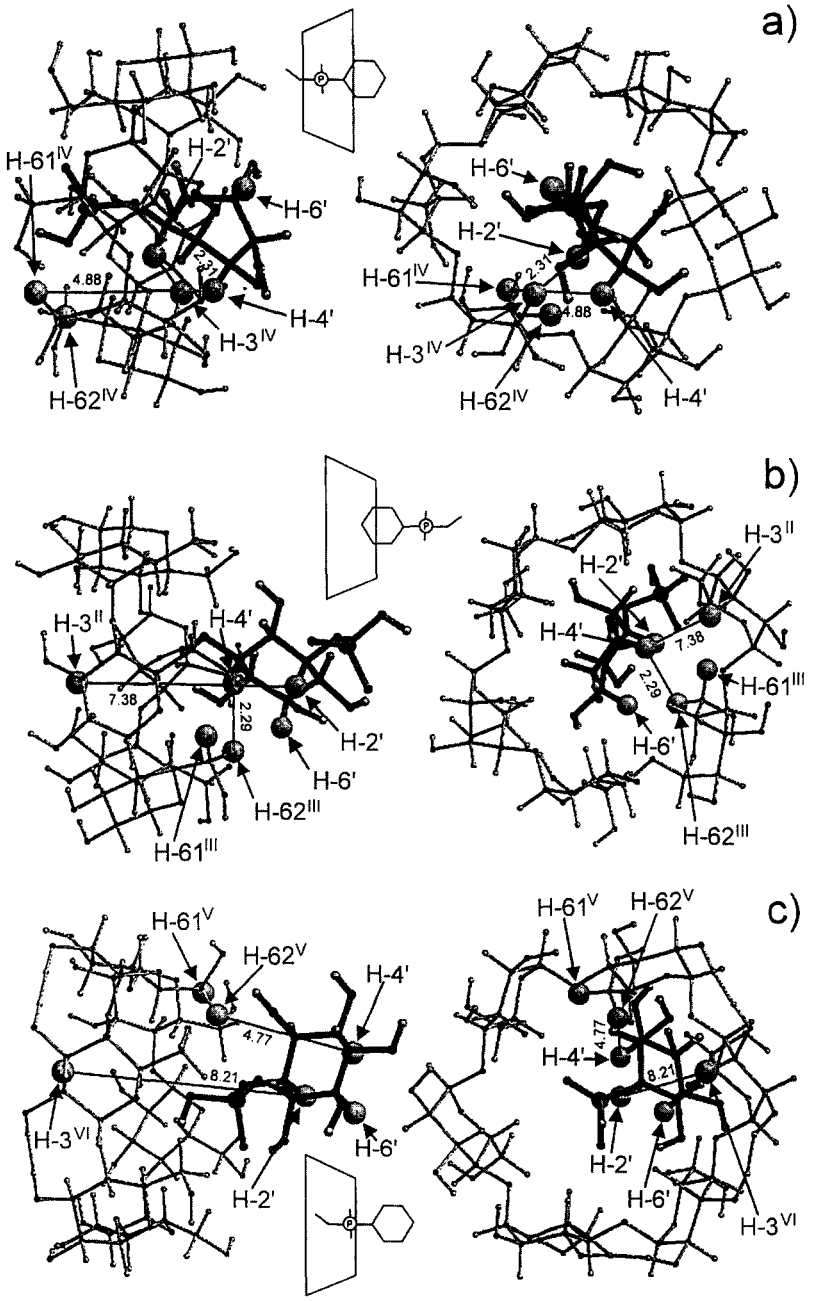

Fig. 5. Possible interaction schemes between α-CD and MY2P. In the upper middle part of each model, the system is sketched with α-CD represented as a truncated cone with its narrow face bearing the primary alcohol function. The corresponding average structures were calculated from 200 ps MD simulations at 300 K in the presence of solvent. (Water molecules have been removed from the figure for clarity.) α-CD and MY2P are drawn with thin and thick sticks, respectively, and hydrogen atoms important in view of NMR results are drawn in CPK. Shortest H–H distances between α-CD and MY2P are shown. (Figure drawn using the molecular graphics program *Molscript* [30].)

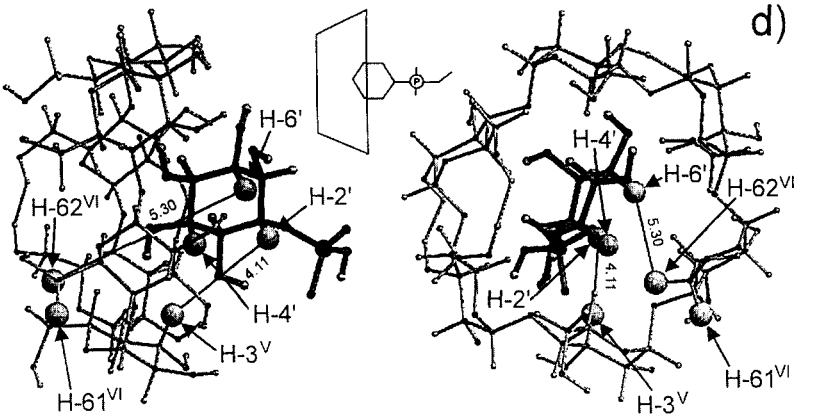

Fig. 5. (continued).

MY2P configuration (a) is the most stable. But when solvation energy is taken into account in E_{Solv}, structures (b) and (d) now have the most negative energies. This is due to the fact that, in these structures, the highly polar phosphate group of MY2P is exposed to the solvent. The total potential energy of the system: E_{Tot}, completely dominated by the unrelevant solvent–solvent interaction energy term, is also given for completeness. From both the NMR and MD results, an attempt can be made to rank the four schemes as follows: (b) corresponds to a stable association between MY2P and the

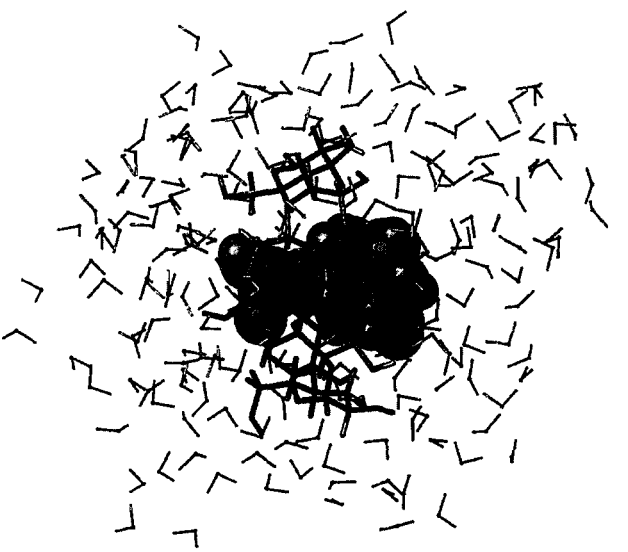

Fig. 6. Snapshot of the solvated system α-CD + MY2P + 201 water molecules are shown in the configuration (a) after 200 ps dynamics at 300 K. A 12 Å solvent boundary potential is applied to the sphere of water molecules. α-CD is shown in wire and MY2P in CPK representation. (Figure drawn using the molecular graphics program *Molscript* [30].)

Table 4
H–H distances shorter than 3 Å

Structure	Solvent		
	α-CD	MY2P	(Å)
(a)	H-3^{I}	H-1′	2.91
	H-3^{II}	H-3′	2.35
	H-5^{II}	H-3′	2.52
	H-3^{III}	H-3′	1.96
	H-3^{III}	H-4′	2.24
	H-5^{III}	H-2′	2.66
	H-5^{III}	H-3′	2.59
	H-3^{IV}	H-2′	2.31
	H-3^{IV}	H-4′	2.26
	H-5^{IV}	H-2′	2.23
	H-3^{VI}	H-1′	2.04
	H-3^{VI}	H-6′	2.60
	H-5^{VI}	H-1′	2.13
(b)	H-61^{I}	H-3′	2.91
	H-5^{II}	H-4′	2.96
	H-62^{II}	H-3′	2.66
	H-61^{III}	H-4′	2.83
	H-62^{III}	H-4′	2.29
	H-62^{III}	H-6′	2.86
	H-62^{V}	H-5′	2.66
	H-62^{VI}	H-5′	2.78
(c)	H-62^{V}	H-3′	2.49
	H-62^{VI}	H-1′	2.32
(d)	H-3^{II}	H-5′	2.35
	H-3^{III}	H-5′	2.48
	H-3^{III}	H-1′	2.84
	H-3^{IV}	H-1′	2.58
	H-3^{V}	H-6′	2.52
	H-3^{VI}	H-6′	2.61

primary hydroxyl side of α-CD and agrees with the experimental nOe observed between H-6 and H-4′; (a) although energetically less favored, is the only one able to explain the experimental nOe observed between H-3 and H-2′. In particular, external association can not account for this measure. This is the case where a tight inclusion complex between α-CD and MY2P is formed (Fig. 6); (d) is the most stable energetically but may be too mobile (facing the «large» secondary hydroxyl side of α-CD) to allow measurable nOe. Table 4, which gives the H–H distances shorter than 3 Å between non-exchangeable protons of α-CD and MY2P, shows seven connectivities for this model, not visible by NMR; (c) is the least likely due to its unfavorable energy and incompatibilities with experimental nOe.

As it is general practice, hydrogen bonds are treated implicitly by CHARMM through electrostatic/VDW interactions so that no extra H-bond energy term is introduced in the

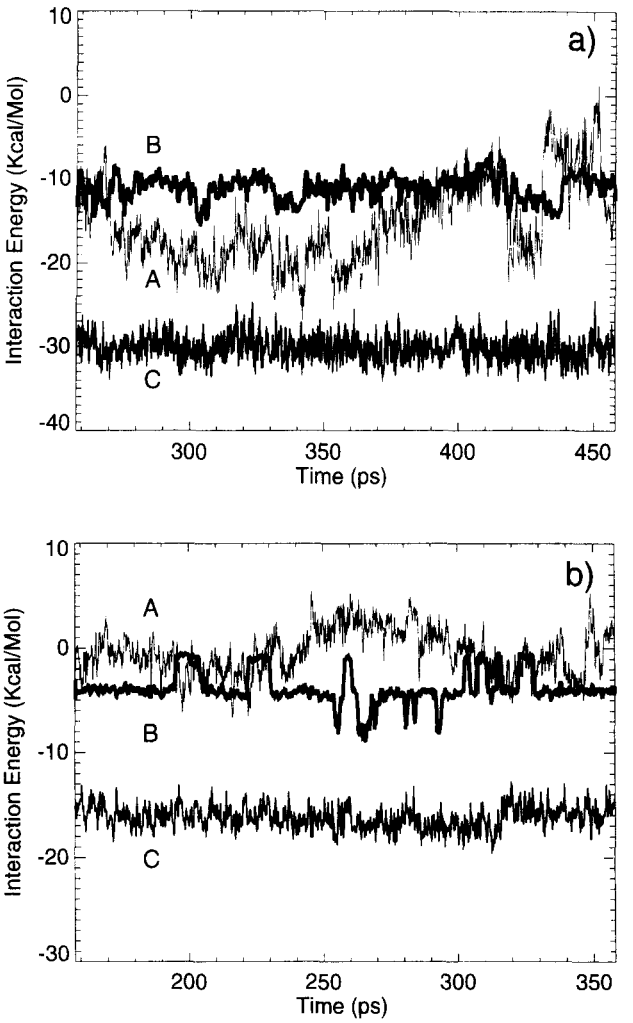

Fig. 7. Decomposition of the interaction energy between α-CD and MY2P The energy is decomposed into the electrostatics (A), H-bonds (B), and VDW (C) contributions during 200 ps MD trajectories in the presence of water at 300 K. H-Bond traces (B) are smoothed by a moving average over two consecutive points. (a) and (b) represent the corresponding initial configurations of the system, shown in Fig. 5a and b.

force field during MD simulations. However hydrogen bond energy terms were calculated explicitly during the analysis of the trajectories following a CHARMM 4–6 potential (well depth: 4.26 kcal/mol, distance: 2.75 Å for oxygens) and 4 Å cutoff. This H-bond energy is plotted in Fig. 7, together with electrostatic and VDW interaction energies between α-CD and MY2P (thus excluding contribution from the solvent). Jumps in the H-bond energy trace correspond to hydrogen bond breaking or reforming. Large fluctuations in the electrostatic energy terms are still visible after 250 ps for model (a), probably due to the interaction between the phosphate group of MY2P and

the OH groups of α-CD. However, the general drift of this energy term seen during the first 200 ps dynamics is absent. This explains why different equilibration times were used for the different configurations. VDW energies of −29.1 (±2.5) and −15.6 (±1.5) kcal/mol for configurations (a) and (b) respectively are the most stabilizing terms.

4. Discussion

In recent years, the hemolytic activity of α-CD has been related to an unspecific extraction of membrane phospholipids [2–12] associated with an inclusion of the lipid side chain. The predominant mechanism induced by this extraction would be an acceleration of the normal exchange cycles (vesiculation) of phospholipids in the natural membranes, with (or without) the creation of a new phospholipid–α-CD compartment in the aqueous medium. The resulting unidirectional flux of the phospholipids would cause severe membrane damages inducing the observable hemolysis. However, our previous work [3] showed a difference in the affinity of α-CD for lipids depending on the nature of the headgroup of the phospholipid. Thus, further studies were undertaken using phosphatidylinositol, the most reactive lipid, in order to determine at a molecular level the mechanism of association of its polar head group: MY2P with α-CD. The chemical shift variations of H-3, H-5 resonances in α-CD and H-2′,1′,3′ in MY2P both suggest an inclusion reaction, an idea consistent with model (a). However, both the absence of stoichiometric data in Job-plots experiments and chemical shift variations of ^{31}P NMR of MY2P in the presence of α-CD contradict a single inclusion. Moreover, in addition to the spatial proximities detected between H-3–5 of α-CD and H-2′ of MY2P — consistent with the inclusion — dipolar correlations are also observed between the protons of α-CD at the narrow side of the torus (H-6) and the H-6′ proton of MY2P. If one considers the negative charge of the phosphorus nuclei and the H-2, H-4 protons of α-CD exposed to the solvent, the conditions for hydrogen bond formation on the outside of α-CD are fulfilled.

From MD simulations, association or inclusion complex between MY2P and α-CD are likely to occur at the primary hydroxyl side of α-CD. However, a configuration showing partial inclusion of MY2P by the secondary hydroxyl side of α-CD, can be found with low energy. Such a sterically 'looser' inclusion allows more conformational freedom for MY2P in the cavity. This may result in a rapid reorientation of MY2P consistent with the absence of detectable nOe corresponding to this conformation. The primary hydroxyl side is also favored in the case of an interaction between α-CD and an inositol phospholipid (PI) as shown by MD free energy calculations [29]. There, it is found that a partial inclusion of MY2P into the secondary hydroxyl side of α-CD is unlikely since, driven by electrostatic forces, α-CD tends to reorient so as to present its primary hydroxyl side to the inositol group. It is also shown that the energy barrier for the reaction: (PI associated to the primary hydroxyl side of α-CD vs. PI fully complexed into α-CD) is less than 15 kcal/mol. Coming back to the present study, possible exchange between MY2P associated to the primary hydroxyl side of α-CD as in (b), and fully complexed as in (a), or rapid reorientation of MY2P at the secondary hydroxyl side

of α-CD as in (d), could both explain the absence of measurable stoichiometry. The relative lifetimes of each of the four possible complexation schemes studied can not be deduced precisely from MD simulations (because the entropic contribution is ignored).

We hope that these experiments will help to improve the understanding of inositol phospholipid–α-CD interactions. The restriction to be pointed out is that the inclusion of phosphatidylinositol by the phosphorus side shall not be considered, due to the presence of the acyl chains and glycerol backbone which do not exist in the case of MY2P. This additional constraint could lead to simpler models of the headgroup–α-CD interactions. However, taking into account classical results [2–8], the inclusion of the acyl chains of phosphatidylinositol is also probable and provides another possibility for phosphatidylinositol–α-CD interaction.

References

[1] I. Sanesama, T. Osajima, and T. Deguchi, *Bull. Chem. Soc. Jpn.*, 63 (1990) 2814–2819
[2] T. Othani, T. Irie, K. Uekama, K. Fuegama, and J. Pitha, *Eur. J. Biochem.*, 186 (1989) 17–22.
[3] F. Fauvelle, J.C. Debouzy, R. Nardin, and A. Gadelle, *Bioelec. Bioenerg.*, 33 (1994) 95–99.
[4] F. Fauvelle, M. Idiri, J.C. Debouzy, A. Gadelle, and R. Nardin, *5éme Réunion du Groupe d'Etudes des Interactions Membranes Molécules*, Rouen (1993) P-3.
[5] Y. Okada, K. Koizumi, K. Ogata, and T. Ohfuji, *Chem. Pharm. Bull.*, 37 (1989) 3096–3099
[6] R.J. Bergeron, M.A. Channing, and K.A. McGovern, *J. Am. Chem. Soc.*, 100 (1978) 2878–2883
[7] P. Job, *Ann. Chim.*, 9 (1928) 113–125.
[8] F. Djedaini, Thèse de Doctorat de l'Université de Paris Sud (1991).
[9] S. Macura and R.R. Ernst, *Mol. Phys.*, 41 (1980) 95–117.
[10] P.C. Manor and W. Saenger, *J. Am. Chem. Soc.*, 96 (1974) 3630–3639.
[11] A.M.C. Miles, D.J. Barlow, G. France, and M.J. Lawrence, *Biochim. Biophys. Acta*, 1199 (1994) 27–36.
[12] I.N. Rabinowitz and J. Kraut, *Acta Cryst.*, 17 (1964) 158–168.
[13] T.R. Lomer, A. Miller, and C.A. Beavers, *Acta Cryst.*, 16 (1963) 264–268.
[14] P.M. Hansbro, S.J. Byard, R.J. Bushby, P.J.H. Turnbull, N. Boden, M.R. Saunders, R. Novelli, and D.G. Reid, *Biochim. Biophys. Acta*, 1112 (1992) 187–196.
[15] B.R. Brooks, R.E. Bruccoleri, B.D. Olafson, D.J. States, S. Swaminathan, and M. Karplus, *J. Comp. Chem.*, 4 (1983) 187–217.
[16] W.F. Van Gunsteren and H.J.C. Berendsen, *Molecular Phys.*, 34 (1977) 1311–1327.
[17] H.J.C. Berendsen, J.P.M. Postma, W.F. Van Gunsteren, A. DiNola, and J.R. Haak, *J. Chem. Phys.*, 81 (1994) 3684–3690.
[18] B.H. Besler, K.M. Merz Jr, and P.A. Kollman, *J. Comp. Chem.*, 11 (1990) 431–439.
[19] M.J.S. Dewar and W. Thiel, *J. Am. Chem. Soc.*, 99 (1977) 4899–4907.
[20] J.E.H. Koehler, W. Saenger, and W.F. Van Gunsteren, *Eur. Biophys. J.*, 15 (1987) 187–210.
[21] W.L. Jorgensen, J. Chandrasekhar, J.D. Madura, R.W. Impey, and M.L. Klein, *J. Chem. Phys.*, 70 (1983) 926–935.
[22] C.L. Brooks III and M. Karplus, *J. Chem. Phys.*, 79 (1983) 6312–6325.
[23] R.J. Bushby, S.J. Byard, P.M. Hansbro, and D.G. Reid, *Biochim. Biophys. Acta*, 1044 (1990) 231–236.
[24] P.M. Hansbro, S.J. Byard, R.J. Bushby, P.J.H. Turnbull, N. Boden, M.R. Saunders, R. Novelli, and D.G. Reid, *Biochim. Biophys. Acta*, 1112 (1992) 187–196.
[25] R. Isnin, H.R. Yoon, R. Vargas, P.A. Quintela, and A.E. Kaifer, *Carbohydr. Res.*, 192 (1989) 357–362.
[26] S. Hashimoto and J.K. Thomas, *J. Am. Chem. Soc.*, 107 (1985) 4655–4662.
[27] D.G. Gorenstein, *Phosphorus 31 NMR: Principles and Applications*, Academic Press, New York, 1984, pp 37–53.
[28] L. Garel, personal communication.
[29] M. Göschl, S. Crouzy, and Y. Chapron, *Eur. Biophys. J., In press.*
[30] P.J. Kraulis, *J. Appl. Chem.*, 24 (1991) 946–950.